ASEAN Engineering Journal

Full Paper

DEVELOPMENT OF A MARKERLESS OPTICAL MOTION CAPTURE SYSTEM BY AN ACTION SPORTS CAMERA FOR RUNNING MOTION

F. Ferryanto[a]*, Andi Isra Mahyuddin[a], Motomu Nakashima[b]

[a]Mechanical Design Research Group, Faculty of Mechanical and Aerospace Engineering, Institut Teknologi Bandung, Bandung, Indonesia
[b]Department of Systems and Control Engineering, Tokyo Institute of Technology, Tokyo, Japan

Article history
Received
23 March 2021
Received in revised form
24 June 2021
Accepted
01 January 2022
Published online
31 May 2022

*Corresponding author
ferryanto@ftmd.itb.ac.id

Graphical abstract

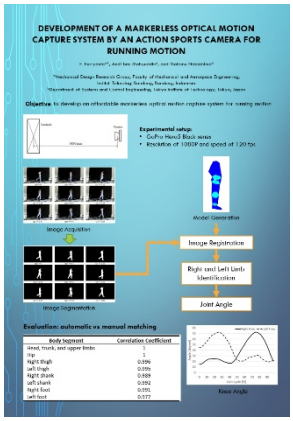

Abstract

A marker-based optical motion capture system is often used to obtain the kinematics parameters of a running analysis. However, the attached marker could affect the participant's movement, and the system is costly because of the exclusive cameras. Due to its drawbacks, the present research aimed to develop an affordable markerless optical motion capture system for running motion. The proposed system used an action sports camera to acquire the running images of the participant. The images were segmented to get the silhouette of the participant. Then, a human body model was generated to provide a priori information to track participants' segment position. The subsequent procedure was image registration to estimate the pose of the participant's silhouette. The transformation parameters were estimated by particle swarm optimization. The optimization output in the form of the rotation angle of the body segment was then employed to identify right or left lower limbs. To validate the results of the optimization, a manual matching was conducted to obtain the actual rotation angle for all body segments. The correlation coefficient between the rotation angle from image registration and the actual rotation angle was then evaluated. It was found that the lowest correlation coefficient was 0.977 for the left foot. It implies that the accuracy of the developed system in the present work is acceptable. Furthermore, the results of the kinematics analysis have good agreement with the literature. Therefore, the developed system, not only yields acceptable running parameters, but also affordable since it uses an action sports camera and easy to use.

Keywords: Action sports camera, Gopro, Kinematics, Markerless optical motion capture, Running

1.0 INTRODUCTION

Running is the oldest sport event since it was started in the first Olympics in 776 BCE. Due to its simplicity and the possibility to perform it anywhere, this sport has become very popular. In the last ten years, running activity has grown around 57% globally [1]. Besides the simplicity, the increase of running activity is also triggered by its benefits, such as health and fitness [2]; and depression and anxiety prevention [3,4].

The growth of running escalates the attention of researchers in running analysis, either biomechanically or physiologically. The running movement is quantified in biomechanics to obtain running parameters, i.e., spatio-temporal, kinematics, and kinetics parameters. The spatio-temporal parameters in the running biomechanics consist of stride length, stride frequency, contact time, flight time, and stride angle [5]. With these parameters, runners' performance could be improved, and the injury could also be prevented. Therefore, biomechanical analysis of running plays an essential part in sports.

The biomechanical analysis of running could be conducted with the help of several systems, such as optical motion capture [6,7], force platform [8,9], or Inertial Measurement Unit (IMU) [10-11]. In the research conducted by Wouda et al., the running movement was represented by the motion of 41 retroreflective markers attached to the participant's skin [6]. This system is called the marker-based optical motion capture system. There are many commercial marker-based optical motion capture systems, for example, Vicon or Optitrack. However, the price is relatively high. One of the efforts to make the system cheaper is the use of Action Sports Camera (ASC). In 2019, Bernardina et al. compared action sports cameras' accuracy for 3D motion analysis with the commercial motion capture system. It was

concluded that the joint angles constructed from the action sports cameras were positively correlated with those obtained from the commercial motion capture system [12].

Even though the application of action sports cameras has cut the cost of a marker-based optical motion capture system, the marker-based system has another disadvantage related to the biomechanical aspects. Those disadvantages are (a) markers attached to the participant could affect the participant's movements, (b) the time required for marker placement could be excessive, (c) the experimental environment must be controlled, and (d) the markers on the skin could move relative to the underlying bone [13]. One of the proposed methods for dealing with those problems is introducing a markerless optical motion capture system. The markerless optical motion capture system has recently been developed to analyze human gait [14] and swimming motion [15,16].

Recently, one of the markerless systems called OpenPose has been developed to detect key points at the body, foot, or hand on single images based on a convolutional neural network [17]. OpenPose could perform gait analysis without the attached marker on the participant's anatomical landmarks. There have been studies that evaluate the accuracy of OpenPose in the gait analysis, such as research conducted by Ota et al. [18] and D'Antonio et al. [19]. Ota et al. compared the joint angles of treadmill walking and running using Vicon and OpenPose. They concluded that OpenPose gave good to excellent agreement of joint angle in the sagittal planes with those obtained from Vicon. However, the joint angle in the frontal plane had a significant error [18]. Moreover, in the study of D'Antonio et al., OpenPose system was inaccurate in the estimation of maxima and minima joint angles compared to IMU [19].

As the result of ASC potential and the drawback of the marker-based optical motion capture system and OpenPose, the present research's aim is to develop an affordable markerless optical motion capture system for running motion. The main contribution of the present work is the affordability of the system because it uses an ASC. Besides, the system is simple and time efficient for the use of coaches and athletes since it does not require markers in the data acquisition. Although it is affordable and simple, the proposed system is also accurate in obtaining the joint angle of the participant. It is expected that athletes could use this markerless system in biomechanical analysis to increase their performances and prevent injury.

2.0 METHODOLOGY

In general, the present method was initiated by an experimental setup to acquire the images of the running movement. After the data acquisition, the method was followed by image segmentation to obtain participant's silhouettes. The silhouettes were used in the image registration to obtain the rotation of angle for each body segment. Prior to image registration, the human body was modeled as eight segments. The model generation was conducted by making use of one frame of running movement images. In the image registration, the model was transformed to have a similar pose to the silhouettes. The last step of the present method was to identify the human body's right and left limbs, especially for lower limbs. The detail of each process is explained below.

2.1 Experimental Setup

The main objective of this work is to develop a markerless optical motion capture system for running movement. To assess the performance of the developed program, an experiment was conducted. The experiment was to video the running movement on a treadmill by an ASC. The running movement was recorded only in the sagittal plane. The camera used in this research was GoPro Hero5 Black series with a resolution of 1080P and speed of 120 frames per second (fps). The ASC was set on a tripod that was separated 385 cm from the center of the treadmill, as shown in Figure 1. The distance of the ASC and the center of the treadmill could be altered on condition that all the body segments are captured in the camera frame.

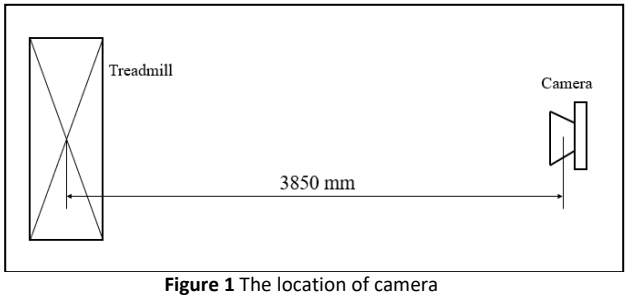

Figure 1 The location of camera

Since the present work's objective is to develop a markerless optical motion capture system, the experiment conducted involved only one male participant. The participant had a body weight of 53 kg and a height of 164 cm. Thus, he had a Body Mass Index (BMI) of 19.7 that could be categorized as normal. The participant also had normal body posture and did not suffer any abnormality, such as scoliosis, lordosis, or kyphosis. Before data acquisition, the participant was dressed in a white outfit to intensify the participant's image contrast to the background. The higher contrast enhanced the accuracy of image segmentation.

Prior to data acquisition, Zhang camera calibration was conducted to obtain the camera parameters. Those camera parameters were used in 2D reconstruction to obtain the kinematics parameter of running motion. In the data acquisition, the participant ran ten cycles on the treadmill with 3.58 m/s speed or 04:39 minutes per kilometer pace while ASC recorded his movement. Although the speed of 3.58 m/s was used in this experiment, there was no limitation regarding the running speed. Basically, the developed system could be used for any running speed. Figure 2 presents the images of running motion recorded by ASC.

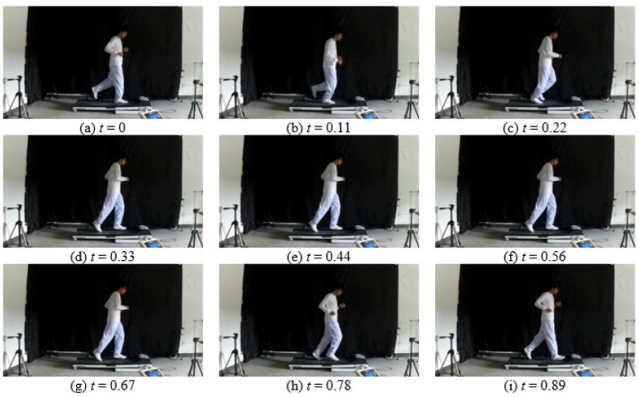

Figure 2 The images of running motion recorded by an action sports camera at 120 frames per second. Each frame was labeled by non-dimensional time normalized by the gait cycle

2.2 Image Segmentation

As shown in Figure 2, the running images captured by ASC were in the Red, Green, Blue (RGB) format. To extract the silhouette of the human body from the background, an image segmentation procedure was conducted. Image segmentation is the process of obtaining the foreground from the background of images. In this case, the foreground was the silhouette of the human body. The silhouette was then used in the process of image registration.

There are many techniques of image segmentation that has been explored by researchers, such as (1) characteristic feature thresholding or clustering, (2) edge detection, and (3) region extraction [20]. In this research, an adaptive background mixture model was applied to obtain the silhouette from the background. This method models each pixel of the image as a mixture of Gaussian distribution [21,22]. The pixel is then classified as either background or foreground based on whether the Gaussian distribution, which represents it most effectively, is considered part of the background model. The advantages of this method were its stability and independent of lighting changes. The result of image segmentation of running images is presented in Figure 3.

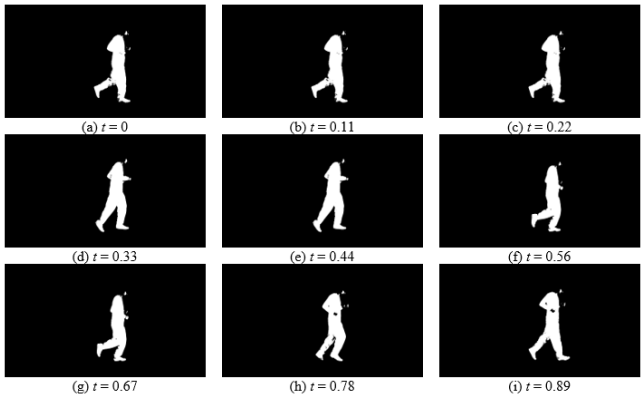

Figure 3 The result of image segmentation of running images. Each frame is in non-dimensional time

2.3 Model Generation

In this research, a model was generated to provide a priori information to track participants' segment position in the running movement. The generated model consisted of participant's body segments that are connected by a corresponding joint. Thus, the preliminary information provided by the model was the transformable kinematics chain. The body segments were transformed to match the pose of running images.

The participant's body was modeled into eight segments and numbered as i = 1 to 8. Those body segments were: (1) Head, trunk, and upper limbs as one segment, (2) Hip, (3) Right thigh, (4) Left thigh, (5) Right shank, (6) Left shank, (7) Right foot, (8) Left foot. The head, trunk and upper limbs were modeled as one segment because the focus of the present research was the biomechanics parameters of lower body. In the model generation, the body segment was segmented and identified manually to enhance the body segment's accuracy. The model generated for the present work is presented in Figure 4. Besides the shape of the body segment, the joint's location was also identified in the model. The location of the joint was selected from the centroid of overlapping area between two segments. For instance, the centroid of the overlapping area of the right thigh and right shank was distinguished as the right knee joint. In Figure 3, the location of the joint is indicated by *.

Figure 4 The generated model as a priori information for image registration. * indicates the location of joint

2.4 Image Registration

After the model generation, the next step in the present method was image registration. Image registration is a process of matching two images obtained in two different times and conditions, one is taken as the reference and the other is the sensed image [23]. The reference image is assumed as static, while the sensed image is an image that is transformed to match with the reference image. In this case, the participant's silhouettes from the image segmentation were the reference images, and the image of the generated model was the sensed image. The image registration's target was to obtain the pose of the body segment that matches with the participant silhouette. Thus, the rotation angle of each body segment could be acquired.

In general, the image registration process is divided into four steps, i.e., feature detection, feature matching, transform model estimation, and image resampling and transformation [23]. The feature is a unique object and could be easily detected in both reference and sensed images. In the present work, the body segment's shape was utilized as the feature because each body segment has a unique shape and could be easily identified in the reference and sensed image. To save the computational time, the shape of body segments was represented by their edge. The edge detection was conducted by the Sobel method [24].

After detecting the feature to be used in the image registration, the reference and sensed images' features were matched. The sensed images' features were transformed by translation and rotation parameters so that the pose of each body segment was similar to those in the reference images. The similarity of pixel intensity value between sensed and reference image was evaluated for each pixel. If the pixel with the same

location between sensed and reference images has the same intensity value, then the pixel similarity increase. Otherwise, if the intensity value of certain pixel between reference and the sensed images is different, then there is no increase of pixel similarity.

As explained before, each body segment in the sensed image was transformed to attain maximum pixel similarity. All the trunk pixel in the sensed image, $\mathbf{x}_1$, was translated by parameter $\mathbf{t} = [t_x\ t_y]^T$ and rotated by rotation angle θ_1 with respect to the trunk centroid. Then, the pixel of other body segments, $\mathbf{x}_i$ with i = 2 to 8, were rotated by an angle θ_i with respect to their proximal joint. The transformation of body segments could be expressed by Equation (1) and (2) below [16].

$$\mathbf{y}_1 = \mathbf{R}(\theta_1)\mathbf{x}_1 + \mathbf{t} \quad (1)$$

$$\mathbf{y}_i = \mathbf{R}(\theta_i)\mathbf{x}_i, \text{ for } i = 2, \dots, 8 \quad (2)$$

where $\mathbf{y}_i$ denotes the pixel position of i^{th} body segment after transformation and $\mathbf{R}(\theta_i)$ is the rotation matrix with angle θ_i.

To ensure the silhouette pose between sensed and reference image was similar, an optimum transformation parameter $\mathbf{T} = [t_x, t_y, \theta_i]^T$ should be evaluated. The optimum transformation parameters could be estimated by minimizing the difference of pixel intensity between sensed and reference image. Mathematically, the transformation parameters were calculated by Equation (3) below.

$$\mathbf{T} = \underset{\mathbf{T}}{\operatorname{argmin}} |\mathbf{m} - \mathbf{d}| \quad (3)$$

where $\mathbf{m} = \{\mathbf{y}_i\}_{i=1}^{8}$ denotes the sensed image or the image of the transformed model and $\mathbf{d} = \{\mathbf{x}_i\}_{i=1}^{8}$ is the reference image. The expression $\underset{\mathbf{T}}{\operatorname{argmin}} |\mathbf{m} - \mathbf{d}|$ is the value of $\mathbf{T}$ that makes $|\mathbf{m} - \mathbf{d}|$ minimum [25]. Equation (3) was solved by particle swarm optimization method [26] available in MATLAB.

In the optimization, the transformation parameters were constrained based on the range of motion of each body segment in the running motion. In addition, the constraint of transformation parameters was also helpful to save the computational cost. The lower and upper boundaries of the optimization constraints were set to – 90 and 90 degrees, respectively for all body segments.

2.5 Right And Left Limb Identification

The image registration procedure's output was the rotation angle of each body segment for the running movement. However, there was no information about the right and left body segment's rotation angle, especially for the upper and lower limb. Therefore, it was necessary to develop an algorithm to identify the rotation angle of the right and left lower limb based on image registration.

The developed algorithm to identify the right and left limb's rotation angle employed a least square approach. The least was acceptable. The rotation angle obtained from the developed system is presented in Figure 6.

distance approach identified the right or left limb based on the next-frame-rotation angle's distance to the rotation angle in the current frame. For example, the right thigh's rotation angle in the current frame classified the closest rotation angle in the next frame as the right thigh. This approach is based on the fact that the body segment in the running movement should move continuously, and it was unlikely to move too fast that the angle difference between two frames was so large for the same body segment.

Besides the angle difference between two consecutive frames, other problems need to be considered in identifying on which side the rotation angle is. Those problems were the angular velocity of the right and left limbs in the current frame. The angular velocity affected the classification because of the inertia principle, i.e., if the right limb rotated counter-clockwise in the current frame, then the right limb's candidate should also move in the counter-clockwise direction for the next frame. Hence, this algorithm needed prior information, such as the right and left body segment's initial rotation angle and their direction.

After identifying the rotation angle for the right and left body segment, the present method then obtain the rotation angle for the occluded body segment, particularly the upper arm, forearm, and hand. A curve-fitting procedure estimated their rotation angles. In this work, the smoothing spline method was exploited with the parameter smoothing of 0.8.

3.0 RESULTS AND DISCUSSION

The smoothed rotation angle obtained from the image matching process was validated by reference data. In this research, the reference data were obtained from the manual image matching. The model was transformed with a pre-developed Graphical user Interface (GUI), as shown in Figure 5. The transformation parameters could be inputted to the textbox to translate and rotate the body segment, and the result of the transformation was observed manually. When the transformed model was perfectly overlapped with the running image, then the transformation parameters were recorded. Those transformation parameters were then called the references.

To confirm the agreement between the rotation angle obtained from image registration and the references, a correlation coefficient between two data was evaluated. The correlation coefficient was ranged from -1 to +1. A good agreement between two data set was indicated by a correlation coefficient's value close to +1. Table 1 shows the correlation coefficient between image registration and the references for the present study. As shown in Table 1, image registration results were correlated with the references with the lowest correlation coefficient of 0.977. These high correlation coefficients implied that the developed markerless optical motion system for running motion in the present work

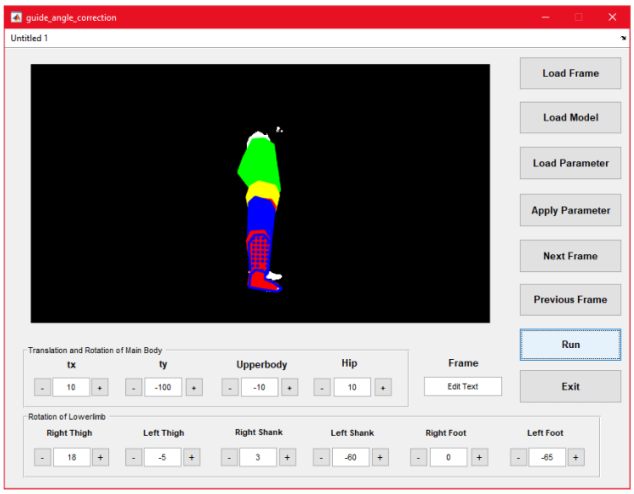

Figure 5 The pre-developed Graphical user Interface (GUI) to help the manual matching procedure in obtaining the actual rotation angle

Table 1 The Correlation Coefficient of Rotation Angle of Body Segment Obtained from the Developed System Compared to the Reference Data

Body Segment	Correlation Coefficient
Head, trunk, and upper limbs	1
Hip	1
Right thigh	0.996
Left thigh	0.995
Right shank	0.989
Left shank	0.992
Right foot	0.991
Left foot	0.977

The rotation angle of each body segment was then used to obtain running parameters, such as spatio-temporal and kinematics parameters. The spatio-temporal parameters of present running motion are presented in Table 2. The parameters were also compared to the result of the Lucas-Cuevas et al. study [5]. It was confirmed that the spatio-temporal parameters of running motion obtained from the developed system were in good agreement with the parameters from Lucas-Cuevas, et al. study. The only different parameter was stride length because the running speed was pre-determined in this study. Hence, the developed markerless optical motion capture was useful in evaluating the spatio-temporal parameters of running motion.

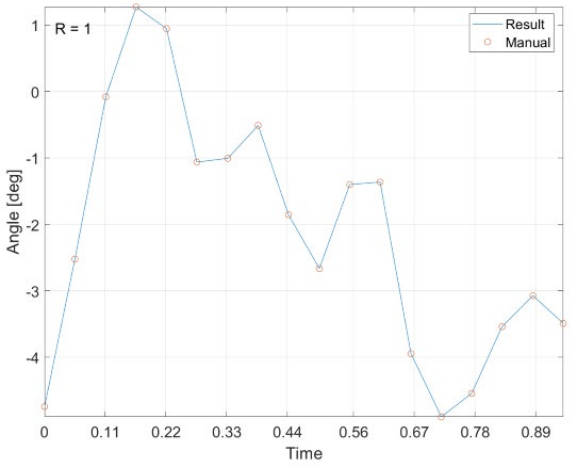

(a) Head, trunk, and upper limbs

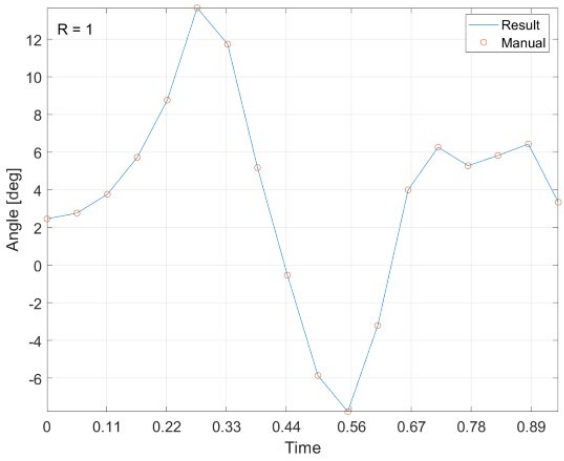

(b) Hip

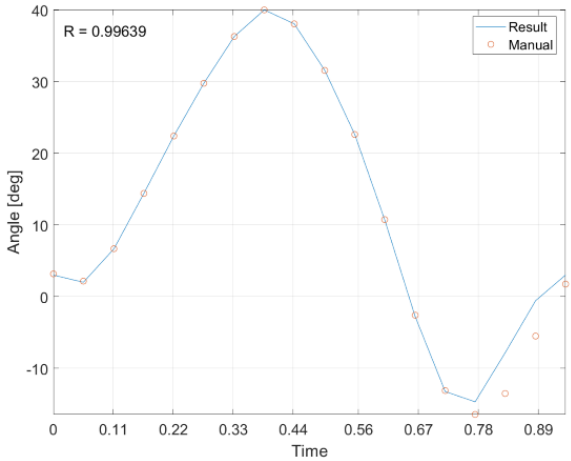

(c) Right thigh

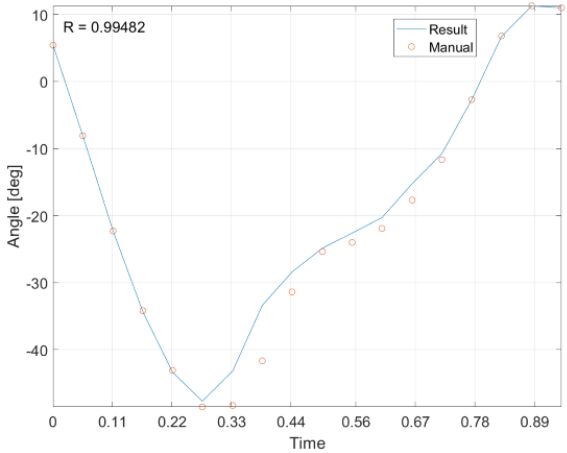

(d) Left thigh

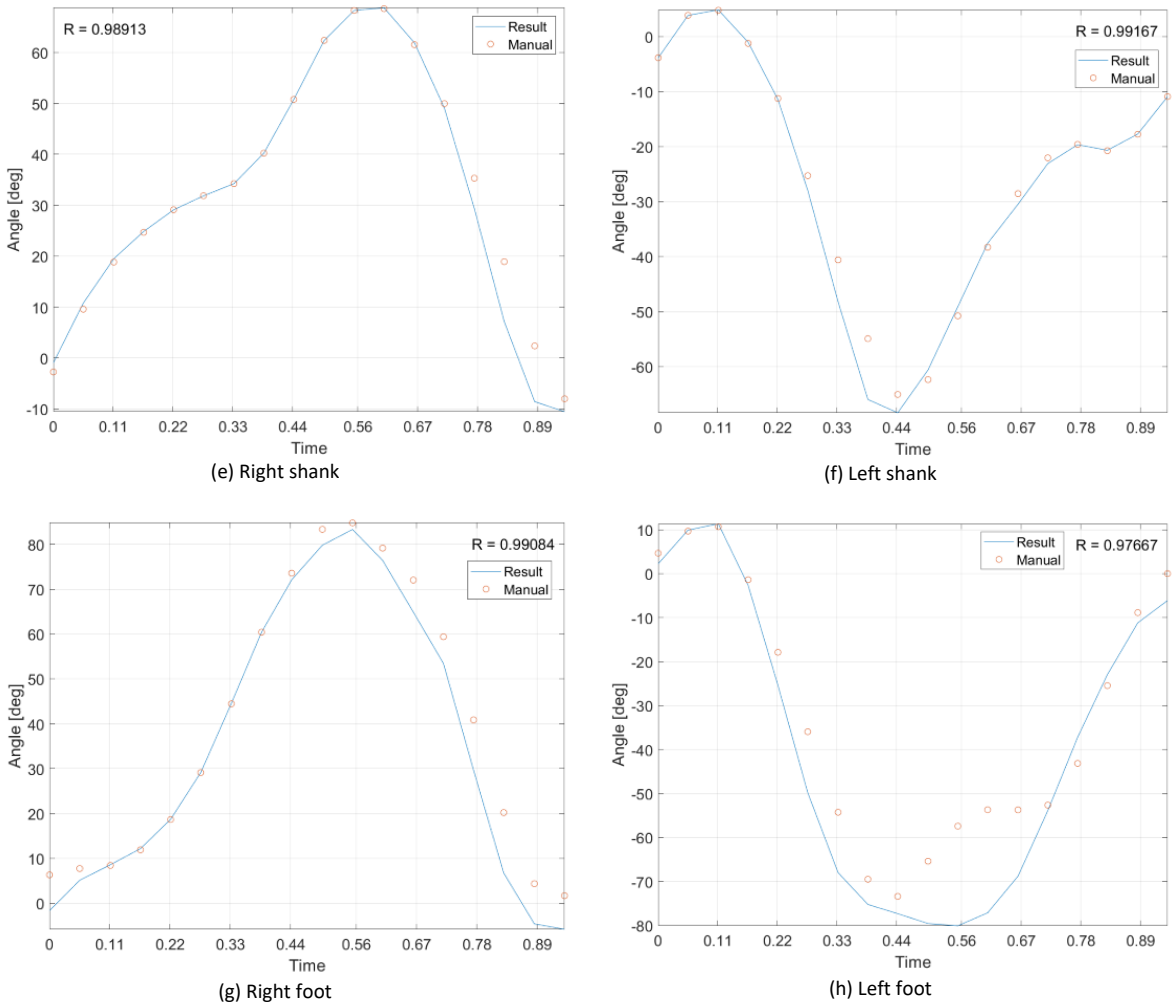

Figure 6 The rotation angle obtained from the developed system compared to the rotation angle obtained from the manual matching: (a) head, trunk, and upper limbs as one segment, (b) hip, (c) right thigh, (d) left thigh, (e) right shank, (f) left shank, (g) right foot, and (h) left foot. The time scale in the *x*-axis corresponds to the running frame of Figure 1

Table 2 The spatio-temporal parameters of present running motion compared to the study of Lucas-Cuevas et al.

Spatio-temporal parameter	Result	Reference [5]
Stride length (m)	3.21	2.25
Stride frequency (Hz)	1.33	1.49
Contact time (s)	0.26	0.24
Flight time (s)	0.11	0.12
Stride angle (degree)	3.14	3.30

Besides the spatio-temporal parameters, kinematics parameters were also investigated to evaluate the advantages of the present system. One of the kinematics parameters investigated in the present study was the joint angle. The joint angle was calculated from the difference of the rotation angle between two body segments. For example, the knee angle is the rotation angle difference of thigh and shank angle. Here, hip, knee, and ankle angles were calculated for both rights and left parts. Figure 7 shows the calculated joint angle. The rotation angle could be further analyzed to obtain kinematics parameters. Therefore, the advantages of the developed system were its affordable price since it uses action sports camera, and ease of use without any need for special configuration in the data acquisition yet yield acceptable running parameters.

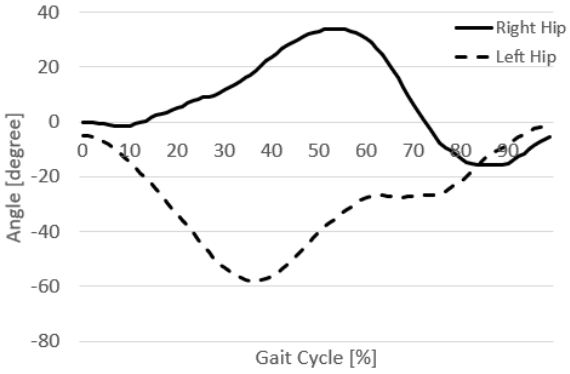

(a) Hip angle

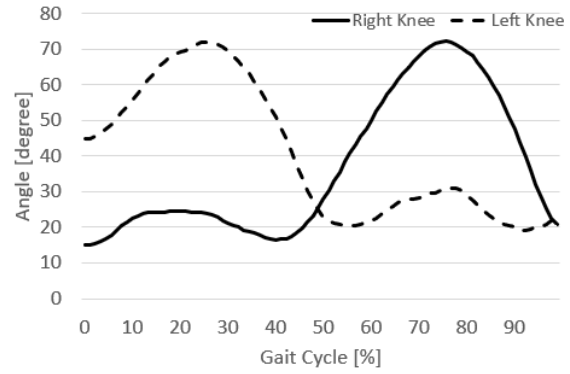

(b) Knee angle

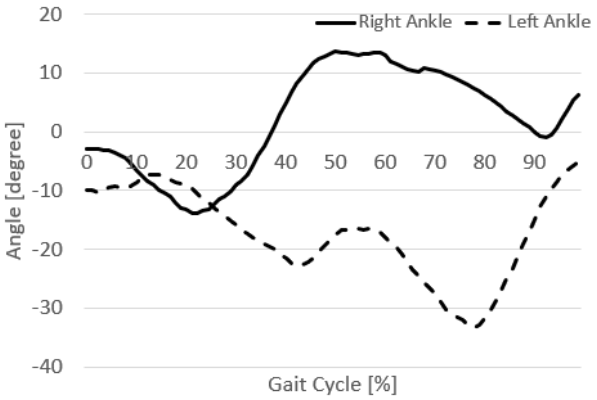

(c) Ankle angle

Figure 7 The calculated joint angle: (a) Hip, (b) Knee, and (c) Ankle

4.0 CONCLUSION

The marker-based optical motion capture system has been widely used in the running analysis. The problem of this system is the high-price, and the attached markers could influence the participant's movement. Therefore, the development of a markerless optical motion capture for running movement was proposed in the present work. The system used an action sports camera to capture the movement of the runner. The images of running movement were segmented into binary images to obtain the silhouettes of the participant. Moreover, the human body was modelled as eight segments, i.e., head, trunk, and upper limb as one segment, hip, right thigh, left thigh, right shank, left shank, right foot, and left foot. The model was transformed translationally and rotationally so that its pose is similar to the silhouettes. The pose similarity was indicated by maximum pixel similarity. Particle swarm optimization was used to maximize the pixel similarity to obtain all the transformation parameters. The obtained transformation parameters were validated by the correlation coefficient to the rotation angle obtained from manual matching. The lowest correlation coefficient was 0.977 for the left foot. It means that the proposed system could be used to obtain the rotation angle of the running analysis. Further analysis was also conducted to obtain the kinematics parameters of running. Since the correlation coefficient was satisfactory, the development of a markerless optical motion capture system was successful. Besides affordable, the system is simple and time-efficient for coaches and athletes since it does not require markers in the data acquisition.

Acknowledgement

The authors gratefully acknowledge the support from the Japan International Cooperation Agency (JICA) for the present study and Aditya Putra Khariza for providing the images of running motion.

References

[1] J. J. Andersen, "The State of Running 2019," 2021. [Online]. Available: https://runrepeat.com/state-of-running.

[2] W. F. Major, 2001. "The Benefits and Costs of Serious Running," *World Leisure Journal*, 43(2): 12-25

[3] L. L. Craft and F. M. Perna, 2004. "The benefits of exercise for the clinically depressed," Primary care companion to the *Journal of clinical psychiatry,* 6(3): 104-111,

[4] V. E. Wilson, B. G. Berger and E. I. Bird, 1981. "Effects of Running and of an Exercise Class on Anxiety," *Perceptual and Motor Skills*, 53(2): 472-472,

[5] Á. G.Lucas-Cuevas, J. I. Quesadaa, JoshGooding, M. G.C.Lewis, AlbertoEncarnación-Martínez and PedroPerez-Soriano, 2018. "The effect of visual focus on spatio-temporal and kinematic parameters of treadmill running," Gait & Posture, 59: 292-297

[6] F. J. Wouda, M. Giuberti, G. Bellusci, E. Maartens, J. Reenalda, B.-J. K. v. Beijnum and P. H. Veltink, 2018. "On the validity of different motion capture technologies for the analysis of running," in IEEE International Conference on Biomedical Robotics and Biomechatronics (Biorob), Enschede, The Netherlands

[7] S. Mihradi, F. Ferryanto, T. Dirgantara and A. I. Mahyuddin, 2013. "Tracking of Markers for 2D and 3D gait analysis using home video cameras," *International Journal of E-Health and Medical Communications* (IJEHMC), 4(3): 36-52

[8] R. Cross, 1999. "Standing, walking, running, and jumping on a force plate," *American Journal of Physics*, 67(4): 304-309

[9] J. H. Challis, 2001. "The Variability in Running Gait Caused by Force Plate Targeting," *Journal of Applied Biomechanics,* 17(1): 77-83

[10] E. Bergamini, P. Picerno, H. Pillet, F. Natta, P. Thoreux and V. Camomilla, 2012. "Estimation of temporal parameters during sprint running using a trunk-mounted inertial measurement unit," *Journal of Biomechanics,* 45(6): 1123-1126

[11] T. H. Jeon and J. K. Lee, 2018. "IMU-Based Joint Angle Estimation Under Various Walking and Running," *Journal of the Korean Society for Precision Engineering*, 35(12): 1199-1204

[12] G. R. D. Bernardina, T. Monnet, H. T. Pinto, R. M. L. d. Barros, P. Cerveri and A. P. Silvatti, 2019. "Are action sport cameras accurate enough for 3D motion analysis? A comparison with a commercial motion capture system," *Journal of Applied Biomechanics*, 35(1): 80-86,

[13] S. Corazza, L. Mündermann, A. M. Chaudhari, T. Demattio, C. Cobelli and T. P. Andriacchi, 2006. "A markerless motion capture system to study musculoskeletal biomechanics: visual hull and simulated annealing approach," *Annals Of Biomedical Engineering,* 34(6): 1019-1029

[14] A. Castelli, G. Paolini, A. Cereatti and U. D. Croce, 2015"A 2D Markerless Gait Analysis Methodology: Validation on Healthy Subjects," Computational and mathematical methods in medicine.

[15] E. Ceseracciu, Z. Sawacha, S. Fantozzi, M. Cortesi, G. Gatta, S. Corazza and C. Cobelli, 2011. "Markerless analysis of front crawl swimming," *Journal of Biomechanics.* 44(12): 2236-2242

[16] F. Ferryanto and M. Nakashima, 2016. "Development of a markerless optical motion capture system for daily use of training in swimming," *Sports Engineering*, 20: 63-72,

[17] Z. Cao, G. Hidalgo, T. Simon, S.-E. Wei and Y. Sheikh, 2019. "OpenPose: Realtime Multi-Person 2D Pose Estimation Using Part Affinity Fields," *IEEE Transactions on Pattern Analysis and Machine Intelligence,* 43(1): 172-186

[18] M. Ota, H. Tateuchi, T. Hashiguchi and N. Ichihashi, 2021 "Verification of validity of gait analysis systems during treadmill walking and running using human pose tracking algorithm," *Gait & Posture*, 85: 290-297

[19] E. D'Antonio, J. Taborri, E. Palermo, S. Rossi and F. Patanè, 2020. "A markerless system for gait analysis based on OpenPose library," in *2020 IEEE International Instrumentation and Measurement Technology Conference* (I2MTC), Dubrovnik, Croatia,

[20] [N. R. Pal and S. K. Pal, 1993. "A Review on Image Segmentation Techniques," *Pattern Recognition*, 26(9): 1277-1294

[21] C. Stauffer and W. Grimson, 1999. "Adaptive Background Mixture Models for Real-Time Tracking," P*roceedings. 1999 IEEE computer society conference on computer vision and pattern recognition (*Cat. No PR00149), 2: 246-252

[22] P. KaewTraKulPong and R. Bowden, 2002"An improved adaptive background mixture model for real-time tracking with shadow detection," in V*ideo-based surveillance systems*, 135-144. Springer,Boston.

[23] B. Zitova and J. Flusser, 2013. "Image registration methods: a survey Barbara," *Image and Vision Computing,* 21: 977-1000

[24] R. C. Gonzalez, R. E. Woods and S. L. Eddins, 2009.Digital Image Processing using MATLAB, United Stalls of America: Gatesmark Publishing.

[25] S. M, "Argmax and Max Calculus," 2016. [Online]. Available:https://www.cs.ubc.ca/*schmidtm/Documents/2016_540_Argmax. pdf. [Accessed 17 February 2021].

[26] R. Poli, J. Kennedy and T. Blackwell, 2007. "Particle swarm optimization," *Swarm Intelligence,* 1(1): 33-57